Mast-Cell Degranulation Induced by Physical Stimuli Involves the Activation of Transient-Receptor-Potential Channel TRPV2

D. ZHANG[1,2], A. SPIELMANN[2], L. WANG[1,2], G. DING[1], F. HUANG[3], Q. GU[1], W. SCHWARZ[1,2,4]

[1]Shanghai Research Center for Acupuncture and Meridians, Department of Mechanics and Engineering Science, Fudan University, Shanghai, China, [2]Max-Planck-Institute for Biophysics, Frankfurt am Main, Germany, [3]State Key Laboratory of Medical Neurobiology, Shanghai Medical College, Fudan University, Shanghai, China, [4]Institute for Biophysics, Goethe University Frankfurt, Frankfurt am Main, Germany

Summary

A characteristic of mast cells is the degranulation in response to various stimuli. Here we have investigated the effects of various physical stimuli in the human mast-cell line HMC-1. We have shown that HMC-1 express the transient receptor potential channels TRPV1, TRPV2 and TRPV4. In the whole-cell patch-clamp configuration, increasing mechanical stress applied to the mast cell by hydrostatic pressure (–30 to –90 cm H_2O applied *via* the patch pipette) induced a current that could be inhibited by 10 µM of ruthenium red. This current was also inhibited by 20 µM SKF96365, an inhibitor that is among TRPV channels specific for the TRPV2. A characteristic of TRPV2 is its activation by high noxious temperature; temperatures exceeding 50 °C induced a similar ruthenium-red-sensitive current. As another physical stimulus, we applied laser light of 640 nm. Here we have shown for the first time that the application of light (at 48 mW for 20 min) induced an SKF96365-sensitive current. All three physical stimuli that led to activation of SKF96365-sensitive current also induced pronounced degranulation in the mast cells, which could be blocked by ruthenium red or SKF96365. The results suggest that TRPV2 is activated by the three different types of physical stimuli. Activation of TRPV2 allows Ca^{2+} ions to enter the cell, which in turn will induce degranulation. We, therefore, suggest that TRPV2 plays a key role in mast-cell degranulation in response to mechanical, heat and red laser-light stimulation.

Key words

Mast cell • Degranulation • TRPV • Physical stimuli

Corresponding authors

W. Schwarz, JWG-University Frankfurt, Institute for Biophysics, Max-von-Laue-Str. 1, Frankfurt am Main 60438, Germany. Fax: (+49) (0)3212 888 3496. E-mail: schwarz@biophys.eu
and
G. Ding, Department of Mechanics and Engineering Science, Fudan University, Shanghai, 200433, China. Fax: (+86) (0)21 5027 3866. E-mail: ghding@fudan.edu.cn

Introduction

Various physical stimuli have been applied to the body surface for medical treatment. These treatments include also those based on traditional Chinese medicine (TCM). The most recognized effect is analgesia in response to mechanical stimulation of selected points close to the body surface (Eshkevari 2003), which are named in TCM acupuncture points (or briefly acupoints). In animal experiments the analgesic effect could be correlated to degranulation of mast cells in the respective acupoints; these points exhibit a particularly high density of mast cells compared to nearby non-acupoints (Zhang *et al.* 2008). The process of mast-cell degranulation is initiated by influx of Ca^{2+} (Sudo *et al.* 1996); in the work presented here we wanted to elucidate which pathway may be activated by mechanical stress applied to the mast cell. Likely candidates in this respect are the stress-sensitive transient-receptor-potential channels (Bíró *et al.* 1998, Stokes *et al.* 2004, Owsianik *et al.* 2006, Ramsey *et*

al. 2006). Human mast cells express the isoform TRPV2; this channel is selectively permeable for divalent cations allowing Ca^{2+} to enter the cell (Gunthorpe et al. 2002). TRPV2 has in addition the exceptional characteristic of being activated by extremely high, noxious temperatures above 50 °C (Numazaki and Tominaga 2004). Such high temperatures are in fact often applied supplementary to the acupuncture needle during moxibustion (Zhang and Wu 2006). Recently, the treatment of acupoints with red laser light has been introduced into the methods of surface treatment in particular in areas of acupoints (Litscher et al. 2000, Litscher 2012). We therefore determined the extent to which TRPV2 could also be activated by this physical stimulus. Part of the results have been previously published in abstract form (Zhang et al. 2007a,b).

Material and Methods

Cell culture and handling

The human leukemia mast-cell line HMC-1 (Butterfield et al. 1988) was kindly provided by Dr. J. H. Butterfield (Mayo Clinic, Rochester, USA). The cells were cultured in 75 cm^2 culture flasks (Corning) containing Iscove's modified Dulbecco's medium (IMDM liquid with L-glutamine, 25 mM HEPES, phenol red, GIBCO Germany) with 10 % heat-inactivated fetal bovine serum (FBS, Biochrom, Berlin, Germany), 4 mM L-glutamine (Biochrom, Berlin, Germany), 100 U per ml penicillin, 100 µg streptomycin per ml (Biochrom, Berlin, Germany) and 0.002 % α-monothioglycerol (Sigma, Deisenhofen, Germany). FBS, L-glutamine, penicillin/ streptomycin and α-monothioglycerol were filtered through a 0.2-µm pore filter. The HMC-1 cells were seeded between 3×10^5 and 1×10^6 cells/ml and split 1:1 every 3-4 days. Incubations were conducted in a humidified incubator at 5 % CO_2 and 37 °C. HMC-1 cells were re-thawed from an original stock every 8-12 weeks.

Western blotting and RT-PCR

In order to determine whether TRPV proteins are expressed in the human mast cells, Western blot analysis as well as conventional reverse transcription PCR (RT-PCR) was performed.

For Western blotting suspensions of HMC-1 ($0.8-1.6 \times 10^7$ cells/ca. 50 ml) were washed twice with 10 ml DPBS (Dulbecco's solution, Invitrogen). The cells were lysed by combined treatment with lysis buffer (50 mM Tris-Cl pH 7.6, 150 mM NaCl, 2 mM EDTA,

1 % Triton, 0.1 % SDS) and sonication for 1 min. Prior to lysis a protease inhibitor cocktail (Sigma) and PMSF (phenylmethylsulfonylfluorid, final concentration 1 mM) was added in order to avoid protein degradation. After centrifugation (two times for 10 min at 20,000 g) supernatants were boiled in SDS buffer for 5 min, resolved by SDS-PAGE (8 %, 5/15 mA, 3 h), and electrotransferred to PVDF membrane. For each Western blot experiment we used 15 µl protein from the same lysate preparation for each lane. The amount of the prepared lysate for those Western blot experiment was 110 µl (55 µl protein lysate with lysis buffer + 55 µl sample buffer). This connoted that every line was loaded by the same amount of protein lysate. The membranes were blocked by 5 % non-fat milk in TBS-T (Tris-buffered saline: 10 mM Tris-HCl, pH 7.4, 150 mM NaCl, 0.1 % Tween 20) for 1 h at room temperature or overnight at 4 °C, and then incubated with the primary antibodies (anti-TRPV1 (VR1 H-150, rabbit polyclonal IgG, Santa Cruz Inc., CA, USA), anti-TRPV2 (VRL-1, H-105, rabbit polyclonal IgG), or anti-TRPV4 (TRPV4, K-18, goat polyclonal IgG, Santa Cruz Inc., CA, USA) for 2 h at room temperature. After three washes with TBS-T the secondary antibody incubation was performed with goat polyclonal to rabbit IgG-H&L (HRP, abcam plc, UK, 0.2 µg/ml) antibody for 1 h at room temperature. Immunoreactive bands were visualized by an enhanced chemoluminescence detection method (ECL Western Blotting Detection Reagents, Amersham Pharmacia Biotech), according to the manufacturer's protocol.

For RT-PCR total RNA was extracted from HMC-1 using Trizol reagent (Invitrogen, Carlsbad, USA). Reverse transcription was carried out using random primers and Moloney murine leukemia virus reverse transcriptase (Promega, Madison, USA). Then PCR was employed for detecting the expression of TRPV1, TRPV2, TRPV4, and β-actin on Mastercycler gradient PCR machine (Eppendorf, Hamburg, Germany). The PCR conditions were: 94 °C 5 min; 94 °C 25 s, 60 °C 25 s, 72 °C 30 s, 33 cycles for TRPV1, TRPV2 and 38 cycles for TRPV4; 72 °C 10 min. RNA extracts from mast cells without reverse transcription served as negative controls. The PCR products were separated on 1.2 % agarose gels. All primers used in PCR are listed in Table 1.

Electrical measurements

Patch-clamp experiments on HMC-1 were performed in the whole-cell configuration using EPC9

Table 1. Sequences of the primers.

Human TrpV1 sense	5' CACCGGTGCCAGGCTGCTGTC 3'
Human TrpV1 antisense	5' GTGCAGTGCTGTCTGGCCCTTG 3'
Human TrpV2 sense	5' GAGTCACAGTTCCAGGGCGAG 3'
Human TrpV2 antisense	5' CCTCGGTAATAGTCATCTGTGC 3'
Human TrpV4 sense	5' CGCCTAACTGATGAGGAGTTTCG 3'
Human TrpV4 antisense	5' CATCCTTGGGCTGGAAGAAGCG 3'
β-actin sense	5' AGCTGAGAGGGAAATCGTGCGTGAC 3'
β-actin antisens	5' ATGTCAACGTCACACTTCATGATGG 3'

equipment with Pulse Software (HEKA, Lamprecht, Germany). Data were sampled at 20 kHz and filtered at 1 kHz. Series resistances and liquid junction potentials were compensated. The holding potential was set in all experiments to –60 mV. Current voltage-dependencies were either determined in voltage-clamp experiments by applying a ramp of 500 ms from –100 to +100 mV, or by applying rectangular 100-ms voltage pulses from –180 to +60 mV (or from –200 to +200 mV) with 20-mV increments. Steady-state currents were calculated from the average of the last 20 ms of the clamp pulse. Membrane capacitance was recorded automatically by the EPC-9 "cap track" feature of the Pulse software together with the extension software of X-chart based on "time domain" technique.

A 0.2-ml perfusion chamber containing the HMC-1 was perfused at 2 ml/min by gravity feed for whole-cell recordings with standard extracellular solution (see Solutions). Recording pipettes were pulled from micropipette glass (GB150T-8P, $1.05 \times 1.50 \times 80$ mm, Science Products GmbH, Germany) on a vertical pipette puller (PP-83, Bachofer GmbH, Germany) to 2-3 MΩ and filled with standard pipette solution (see Solutions).

Methods of stimulating cell degranulation

To apply mechanical stress to the mast cells, negative pressure of –30, –60 or –90 cm H_2O was supplied to the patch pipette. Occasionally positive pressure of same magnitude was supplied, which showed similar effects. For measurements on suspensions of intact cells mechanical stress was applied by hypoosmotic solution (see Solutions) of 240 mOsm compared to 310 mOsm of standard soltution.

For thermal stimulation of the HMC-1 the chamber was perfused with preheated solution. The temperature of the solution was controlled by a Peltier Temperature Control Device (PTC-20, NPI, Tamm, Germany). The temperature was monitored by a thermistor at the position of the cell under investigation.

Red light of 640 nm was supplied by a semiconductor laser (Litscher and Schikora 2007). The equipment was kindly provided by Dr. D. Schikora (University of Paderborn). The light guide with an output energy of 48 mW and an output power density of about 6 W/cm^2 was positioned at a distance of 8 mm from the cell. Since light of 640 nm is poorly absorbed by water, the laser light could not have induced major temperature changes. Direct measurements confirmed that irradiation of 20 min resulted in a temperature increase of no more than 0.5 °C. The effect of laser irradiation on mast cells was microscopically observed using Axiophot (Zeiss) microscope and Powershot G5 camera (Cannon); pictures were taken every 5 minutes at a magnification of ×100 and camera digital enlargement at ×2.0. Each picture was taken with the laser switched off, and Image J software was used to measure cell perimeters and areas.

Fluorescence measurements

For determination of fluorescence intensity in HMC-1 the cells were grown on glass cover slips coated with poly-L-lysine (Sigma Chemical Co.) for 10 min, and then loaded with 4 μM Calcium Green-1 AM in IMDM loading buffer for 30 min. Thereafter, the cells were washed three times with standard extracellular solution and placed in a perfusion chamber on the stage of an inverted microscope (Nikon, TE2000-U). A 100-W super high pressure mercury lamp (Nikon, C-SHG1) was used as a light source. The excitation light was passed through an interference filter (465-495 nm) and reflected by a dichroic mirror (cut-off wave lengths 505 nm) through a 40x plan objective. Filter and dichroic mirrors were from Nikon. Fluorescence images were collected by an

intensified CCD video camera (Hamamatsu, ORCA-ER). Images were digitized and averaged (5 frames), background-corrected, stored every 1 minute, and analyzed by an image-processing system (Wasabi). Fluorescence intensities of individual cells in the field of view were determined by averaging the image intensity collected from regions of interest within each cell. All experiments were performed at room temperature.

Measurements of histamine release

To illustrate mast cell degranulation by physical stimulation we measured release of histamine from HMC-1 into standard extracellular solution. The cells were divided into seven groups: untreated controls, and cells treated by hypotonicity, heat, or laser light with and without 20 µM SKF96365 (stimulations were as described before). The cell solutions (with density of $2×10^5$/ml) were centrifuged at 3000 revolutions per minute for 5 min and the supernatants were collected. To aliquots of 1 ml supernatant 0.5 ml NaOH (0.4 M) and 0.1 ml o-phthaldialdehyde (0.05 %) were added to stabilize the fluorescence. After 10 min the samples were neutralized by adding 0.5 ml HCl (0.1 M). The cell pellets were resuspended in 2 ml standard extracellular solution and boiled at 100 °C for 5 min. Lyses solution was collected after the centrifuge as described before for the supernatant. Fluorescence intensity in cell supernatants and lyses solutions was determined by fluorescence spectrometer (Hitachi, F-4500) (λ_{ex}=350 nm, λ_{em}= 440 nm). Released histamine was calculated as the ratio of fluorescences (F)

$$F_{supernatant}/(F_{supernatant} + F_{lyses})*100$$

Data analysis

Electrophysiological data from the Pulse program and fluorescence intensity data were exported in ASCII format to Origin software (ADITIVE, Friedrichsdorf, Germany) for further analysis and presentation. Averaged data are presented as mean ± S.E.M. Data were considered as statistically significant different on the basis of $p<0.05$ using Student's t-test of the Origin software.

Solutions

Standard extracellular solution contained (in mM) 150 NaCl, 5 KCl, 2 CaCl$_2$, 5 MgCl$_2$, 4 D-Sorbitol, 10 Hepes, pH7.4 (adjusted with NaOH). Hypo-osmotic solution was prepared by reducing the NaCl concentration to 100 mM and maintaining the other constituents as in standard solution. Standard pipette solution contained (in mM) 140 CsCl, 1 CaCl$_2$, 2 MgCl$_2$, 15 Hepes, 5 EGTA, pH7.2 (adjusted with Tris).

Stock solutions of the inhibitors Ruthenium Red and SKF96365 (1 M in distilled water) or disodium chromoglycate (DSCG, 1 g/ml in distilled water) were diluted in external solution to the final concentration of 10 µM and 20 µM or 20 mg/ml, respectively. The solution with the inhibitors RuR and SKF96365 were delivered by a pressure-driven perfusion system (DAD-VC-8, ALA Scientific Instruments Inc.) with its tip positioned about 50 µm away from the cell being recorded to ensure that the cell was fully within the stream of the perfusate.

For investigation of cation (magnesium/cesium) permeability ratios of mechano-activated channels, the bath solution was changed to solutions containing as divalent cations 1, 5, 20 or 50 mM MgCl$_2$ with 166, 160, 135 or 95 mM TMA-Cl, respectively, and 10 mM HEPES, pH7.2 (adjusted with Tris). The composition of the pipette solution was 160 mM CsCl, 1 mM MgCl$_2$, 14 mM HEPES, 5 mM EGTA, pH7.2 (adjusted with Tris).

Results

HMC-1 express TRPV2

Mast cells have been demonstrated to express transient receptor potential channels of the TRPV family for various types (see e.g. Bradding *et al.* 2003). To demonstrate that TRPV proteins are also present in the human mast cell line HMC-1, Western blot analysis was performed. Figure 1A shows that not only TRPV2 (VRL-1) (86 kDA) is expressed in HMC-1 but also TRPV1 (VR1) (95 kDA) and TRPV4 (VRL-2) (85 kDA). In lysates of HMC-1 cells, anti-TRPV1 and anti-TRPV2 immunoreactivity appeared as multiple bands. In addition, we performed reverse transcription PCR, demonstrating the expression of TRPV1, TRPV2 and TRPV4 in the HMC-1 (Fig. 1B). Both Western blot and RT-PCR indicate that TRPV1, TRPV2, and TRPV4 are expressed in HMC-1. In the subsequent studies we focused on TRPV2.

Mechanical stress activates TRPV2 and induces degranulation

The cell membrane was subjected to mechanical stress by applying negative pressure through the patch
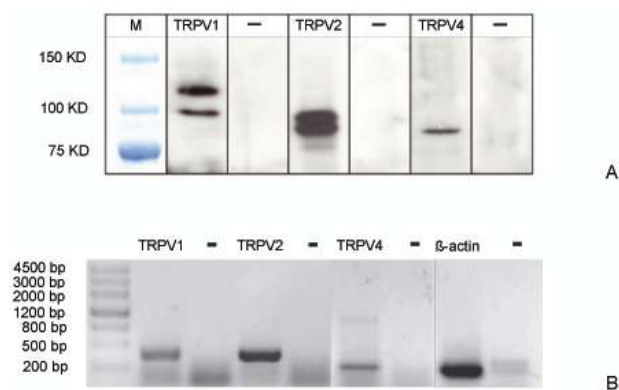
Fig. 1. Expression of TRPV1, TRPV2 and TRPV4 in Human Mast Cell Line 1 (HMC-1). **(A)** Western blots of HMC-1 lysates with anti-TRPV1, anti-TRPV2, and TRPV4; as negative controls, indicated by the -, lysates of *Xenopus* oocytes treated in the same way were used. **(B)** RT-PCR of RNA extracted from HMC-1 for detection of TRPV1, TRPV2, TRPV4, and as a control β-actin; RNA extracts without RT served as a negative control (-).

pipette in whole-cell configuration. At a pressure of -60 cm H_2O an inward-directed current developed that reached a maximum after about 15 s and slowly decayed thereafter (Fig. 2A). The current response could be blocked by 10 μM Ruthenium Red (RuR); in the presence of RuR only a very small current could be induced by the pressure gradient.

Current-voltage dependencies were obtained by the application of voltage ramps (indicated by the vertical deflections in Fig. 2A). Averaged current-voltage curves are shown in Figure 2B. At 10 μM RuR the current became significantly reduced. The RuR-sensitive, stress-activated current component exhibited a reversal potential at $+15$ mV (see inset Fig. 2B). The current was hardly voltage-dependent within the potential range covered.

The application of mechanical stress was associated with mast cell degranulation. Figure 2C shows as an example the effect of hypoosmotic stress. Data in Table 2 demonstrate the degranulation by hypoosmotic-stress-induced histamine release. Degranulation could also be detected in whole-cell configuration after applying a pressure gradient. Degranulation could be effectively blocked by 20 μM SKF96365 which is among the TRPV family a specific inhibitor for TRPV2 (Clapham 2009); an example is shown in Figure 2D. The 40 % inhibition by 20 μM SKF96365 indicates that TRPV2 activation contributed to the degranulation process. In contrast to SKF96365, RuR inhibits not only TRPV2, but also other channels, in particular other

members of the TRPV family (Gunthorpe *et al.* 2002). The more specific inhibitor SKF96365 at 20 μM blocked not only the pressure-induced degranulation but also the current became significantly reduced (Fig. 2E). Mechanical stress induced also a current component that was insensitive to RuR and SKF96365 (Fig. 2A, B and E). The current remaining in the presence of the inhibitors is still significantly larger than that under control conditions.

Table 2. Effect of physical stimuli on histamine release ratio. Data represent averages of 3 samples ± S.E.M. Means are significantly different on the basis of ▲p<0.01 vs control; Δp<0.01 vs. respective group without SKF96365.

Groups (n=3)	Histamine release ratio in the absence of SKF96365 (%)	Histamine release ratio in the presence of 20 μM SKF96365 (%)
Control cells	13.9 ± 1.6	12.9 ± 1.3
Hypotonic solution (240 mOsm)	79.5 ± 2.3▲	49.1 ± 2.6▲Δ
Heat application (53 °C by perfusion)	88.3 ± 2.0▲	36.0 ± 2.4▲Δ
Laser irradiation (48 mW)	65.0 ± 2.9▲	35.4 ± 3.5▲Δ

Figure 2F illustrates stress-induced single-channel events. Single-channel analysis in the outside-out membrane patches revealed outward rectifying, RuR- and SKF-insensitive events. The single-channel conductance at positive potentials (50 pS) strongly depends on Cl^- concentration indicating that this pressure-activated current component may be mediated by Cl^- channels.

Increasing the amplitude of negative pressure from -30 to -90 cm H_2O resulted in increasing currents as illustrated for the holding current at -60 mV (Fig. 2G). Application of 30 cm H_2O negative pressure did not produce significant activation compared to the base level, while 60 and 90 cm H_2O negative pressure both induced large currents.
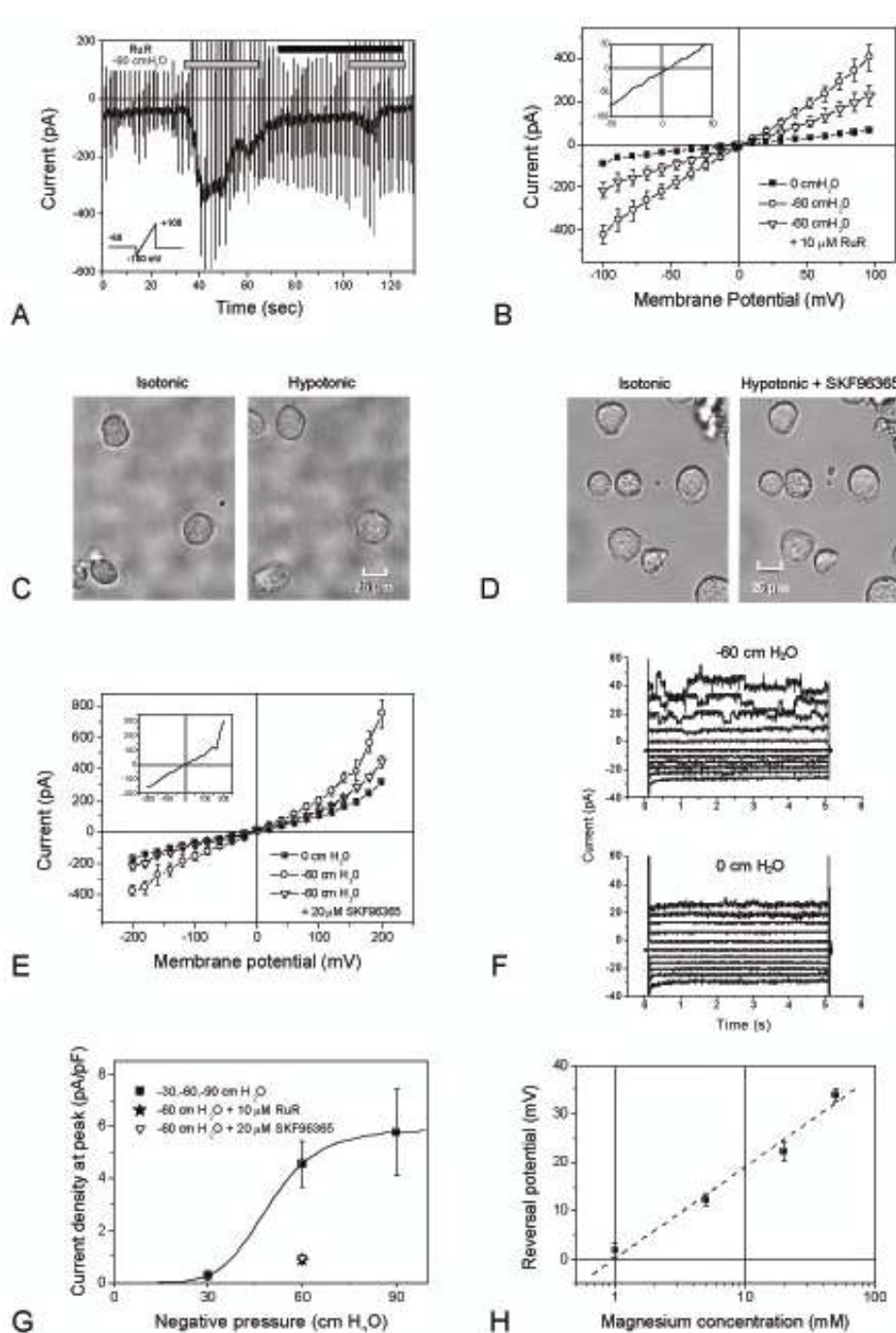
Fig. 2. Dependence of membrane currents on mechanical stress. **(A)** Chart recording in whole-cell mode at holding potential −60 mV. Voltage ramps from −100 to +100 mV were applied every 2 s. The resulting currents are shown as vertical deflections. Negative pressure of 60 cm H_2O was supplied to the patch pipette (grey bars) in the absence or in the presence (black bar) of 10 µM RuR. **(B)** Voltage dependence of currents induced by mechanical stress. Voltage ramps were applied in whole-cell mode before (0 cm H_2O) and at the maximum response during −60 cm H_2O pressure gradient in the absence (open circles) and the presence (open triangles) of 10 µM Ruthenium Red (compare Fig. 2A). Data represent averages of 10 experiments (± S.E.M.) (p<0.05). The inset shows 10 µM RuR-sensitive component of the stress activated current. **(C)** Degranulation in response to hypoosmotic stress (310 mOsm to 240 mOsm by decreasing NaCl from 140 mM to 100 mM in the bath solution). **(D)** Block of hypoosmotic induced degranulation by 20 µM SKF96365. **(E)** Rectangular voltage pulses of 200 ms duration were applied in whole-cell mode before (filled squares) and at the maximum response during −60 cm H_2O pressure gradient in the absence (open circles) and presence (open triangles) of 20 µM SKF96365 and steady-state currents were determined. Data represent averages of 5 experiments (± S.E.M.) (p<0.05). **(F)** Current traces in response to 5 s voltage pulses applied to outside-out patches from −100 to +100 mV in 20 mV increments (applied from 0 mV). Lower trace at 0 cm H_2O, upper traces at −60 cm H_2O pressure. **(G)** Pressure dependence of maximum current density. Current densities (determined in whole-cell mode as the ratio of current and cell capacitance) at the holding potential of −60 mV with increasing negative pressure from −30 to −90 cm H_2O. Filled squares in the absence, the filled star in the presence of 10 µM RuR, and open triangle of 20 µM SKF96365. The solid line is an arbitrary fit suggesting half-maximum stimulation at about −50 cm H_2O. Data are averages from 5 experiments (± S.E.M.). Current density at −60 cm H_2O is significantly different from the current density at −30 cm or in the presence of one of the two inhibitors (p<0.05), but not to −90 cm. **(H)** Reversal potential of mechanical-stress-activated current. Reversal potentials of pressure induced whole-cell currents were determined at different Mg^{2+} concentrations in the bath solution ($MgCl_2$ replacing equiosmolarly TMACl). The pipette solution in the whole-cell configuration contained 160 mM CsCl. Data represent averages of 5 experiments (± S.E.M.). The dotted line is a linear fit in the logarithmic scale with a slope of 19 mV per 10-fold change in Mg^{2+} concentration. For symbols without visible error bar the error is within the symbol size.

TRPV2 is a divalent cation-permeable channel (Gunthorpe *et al.* 2002). Changing the Mg^{2+} concentration in the external bath solution shifted the reversal by 19 mV per 10-fold change in the Mg^{2+} concentration (Fig. 2H). This is clearly less than the 29 mV expected for a divalent cation-selective channel, and may be attributed to a contribution of the Cs^+ (160 mM) in the pipette solution. For determination of cation permeabilities, cells were bathed with extracellular solutions containing the respective divalent cation X^{2+}

(Mg^{2+}, Ca^{2+} or Ba^{2+} at 100 mM) with the pipette solution containing Cs^+ (160 mM). Depolarising ramp pulses were applied as described before, at the peak of current induced by –60 cm H_2O, to obtain the reversal potentials in the respective bath solutions. The reversal potentials for the three divalent cations did not differ significantly. Based on a modified GHK equation including divalent cation permeability ratios with Cs^+ as the only permeating internal ion, P_X^{2+}/P_{Cs}^+ values were calculated as

$$P_X^{2+}/P_{Cs}^+ = [Cs^+]_i \exp(\Delta V_{rev} F/RT)(1+\exp(\Delta V_{rev} F/RT))/4[X^{2+}]_o,$$

where the bracketed terms are the ion activities, V_{rev} the reversal potential; F, R and T stand for Faraday constant, gas constant and absolute temperature as usual. The relative permeability ratios were 3.46, 4.55 and 3.74 for Mg^{2+}, Ca^{2+} and Ba^{2+}, respectively.

Temperatures above 50 °C activate TRPV2 and induce degranulation

Increasing the temperature of the bath solution surrounding the cells induced an inward-directed current only at temperatures exceeding 50 °C (Fig. 3A). This is a characteristic of TRPV2. As with the response to mechanical, this temperature response could be blocked by 10 µM RuR. Experiments with SKF96365 were not performed since the high temperature threshold is already specific for TRPV2. Figure 3B shows the effect of 53 °C; even at 45 °C only a very small, though significant current increase could be detected. The complete inhibition by RuR for the current over the entire voltage range illustrates that in contrast to the mechanical stress-induced current, the heat-induced current shows no additional RuR-insensitive component. For the voltage range used in the experiments with pressure changes (–100 to +100 mV), the heat-activated current also exhibited nearly linear voltage dependence. Only at the more negative potentials the inward rectification became apparent. Figures 3C and 3D illustrate with specific examples that heat does indeed leads to a degranulation event that can be blocked by SKF96365. Also the heat-induced histamine release and its strong inhibition by 59.2 % demonstrates TRPV2 involvement in the degranulation process (Table 2).
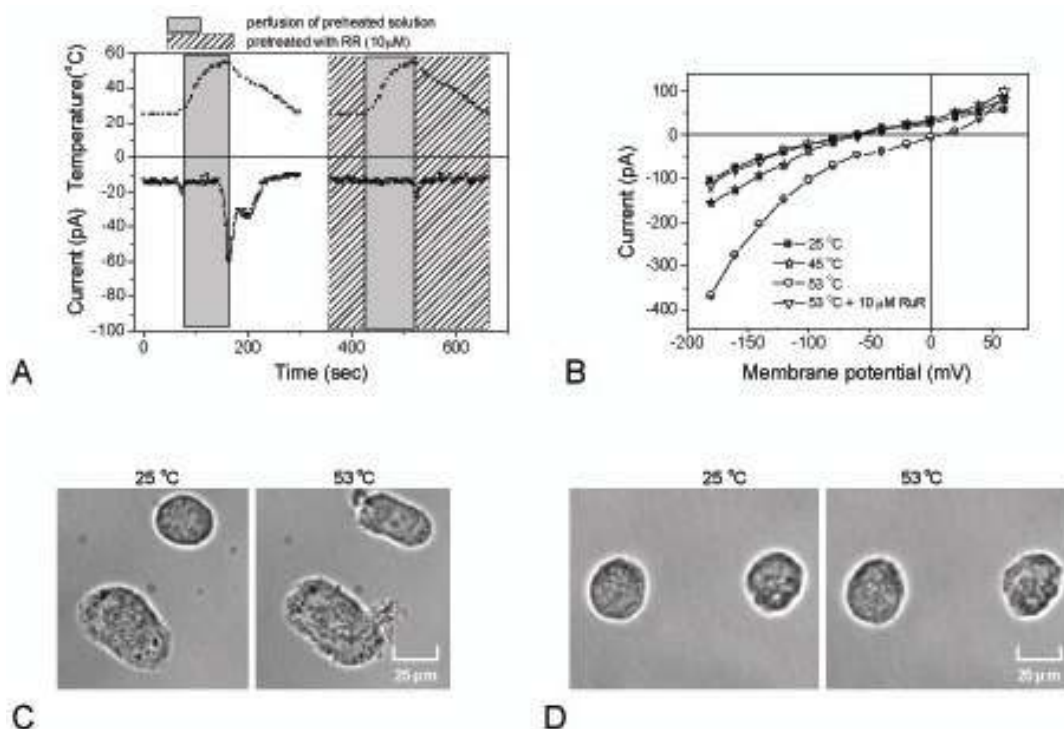
Fig. 3. Activation of an inward-directed current by high temperature. **(A)** Whole-cell recording at a holding potential of –60 mV (lower traces) in the absence (left) and presence of 10 µM RuR (right). Temperature changes were achieved by perfusion of the test chamber with preheated solution. The temperature was measured by a thermistor at the position of the cell (upper traces). **(B)** Effect of heat application on current-voltage dependencies. An inwardly rectifying current in whole-cell mode is activated at temperatures exceeding 50 °C (open circles) compared to the current at 25 °C (filled squares) and 45 °C (open stars). The signal is completely blocked by 10 µM RuR (open triangles). Data represent averages from 3 experiments (± S.E.M.) (p<0.05). **(C)** Heat-induced (53 °C) degranulation observed under light microscopy; left before heat application, right after. **(D)** Block of degranulation by 20 µM SKF96365; left before heat application, right after. For symbols without visible error bar the error is within the symbol size.
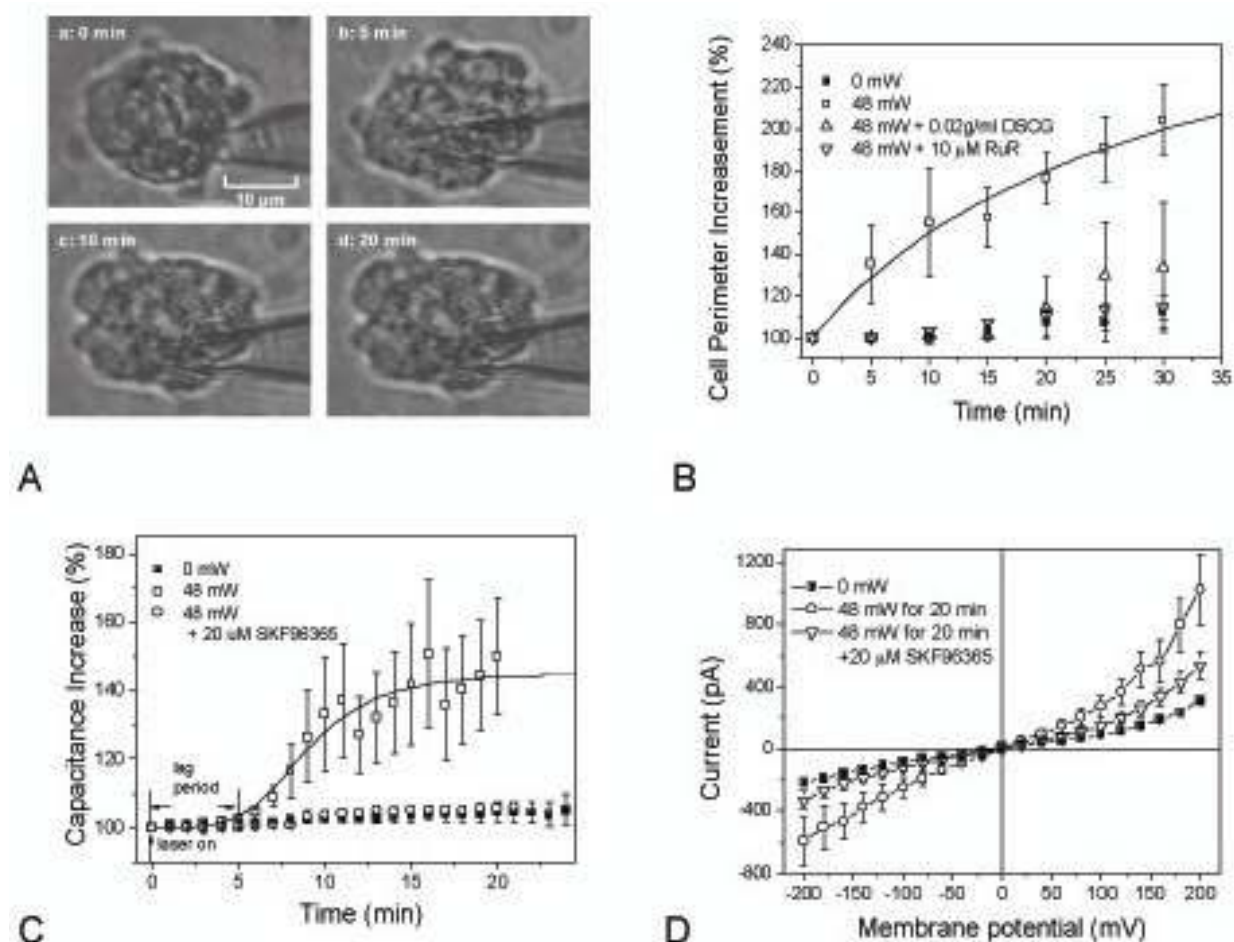
Fig. 4. Effect of laser stimulation (640 nm, 48 mW). **(A)** Mast cell degranulation induced by laser stimulation. **a:** Initial status of a mast cell attached to a patch pipette; the picture was taken after formation of a GΩ seal in the whole-cell mode. **b, c,** and **d:** same cell as in **a,** but photographed 5, 10, and 20 min after the start of laser stimulation. Scale bar=10 μm. **(B)** Cell perimeter as a measure of degree of degranulation. Data are expressed as a percentage of perimeter under laser irradiation (open squares), pretreatment for 10 minutes with 20 mg/ml DSCG (triangle up) or 10 μM RuR (triangles down). Cells without irradiation are shown as filled squares. Data represent averages from 6 experiments (± S.E.M.); for time ≥ 10 min the data are significantly different to those without irradiation (p<0.05). **(C)** Laser-induced capacitance increase. During the laser radiation at 48 mW, the membrane capacitances in whole-cell mode increased (open squares) after a lag period of about 5 min; open circles are data obtained in the presence of 20 μM SKF96365. Cells without irradiation are shown as filled squares. Data represent averages of 5 cells from 2 batches (± S.E.M.); for time ≥ 9 min the data are significantly different to those without irradiation (p<0.05). **(D)** Current-voltage dependence of current activated by laser light. Current-voltage dependencies in whole-cell mode were determined as the difference of current before (filled squares) and after (open circles) 20 min of illumination. Open squares represent data without and open circles with 20 μM SKF96365, and are averages of 5 experiments (± S.E.M) (p<0.05). For symbols without visible error bar the error is within the symbol size.

Light of 640-nm activates TRPV2 and induces degranulation

When mast cells were illuminated with 640-nm laser light, they started to degranulate after a lag phase of about 5 min. Figure 4A illustrates by light microscopy the progressive development of mast-cell degranulation during a whole-cell patch-clamp experiment. To study the progressing degranulation we observed the cells under the microscope and determined the cells' perimeter as a measure of the extent of degranulation (Fig. 4B). Degranulation could be blocked not only by the membrane stabilizer DSCG (20 mg/ml), but also by the TRPV inhibitor RuR. A more accurate indicator of degranulation is the altered membrane capacitance that

can be followed during a whole-cell voltage-clamp experiment (Fig. 4C). Despite the large variability among different cells, a clear and significant (p<0.05) increase in capacitance was detectable.

The increase in capacitance was also accompanied by a significant increase in membrane conductance (Fig. 4D). Application of SKF96365 (20 μM) blocked the light-induced current and also counteracted the degranulation. The results demonstrate that this current was mediated by TRPV2 as inhibition of TRPV2 blocked the degranulation. The light-induced histamine release and its 45 % inhibition demonstrate TRPV2 involvement in the degranulation process.
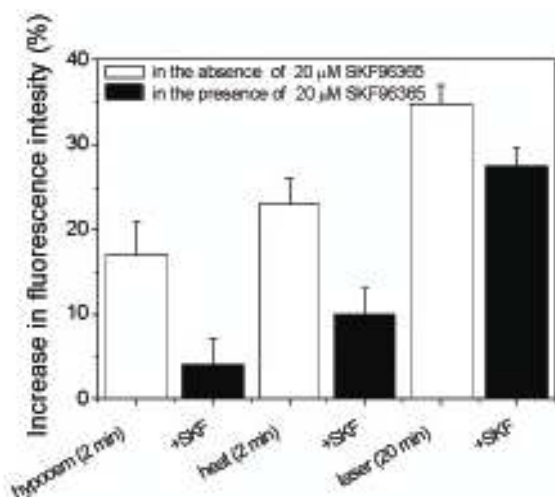
Fig. 5. Changes in fluorescence intensity of the Ca-sensitive dye (Calcium Green-1AM) after mast cell stimulation by osmotic stress, noxious heat (53 °C) and red laser light. Open bars represent values in the absence of 20 µM SKF96365, filled bars in the presence. Data of n=7 are represented as mean ± S.E.M. The inhibition by SKF96365 was significant after osmotic stress, heat and laser light (p<0.01).

Mechanical, thermal and laser light stimulation result in SKF96365-sensitive Ca^{2+} entry

The transmembrane pressure-induced activation of SKF-sensitive current could also be achieved by osmotic stress (not illustrated). The induction of the current was associated with an increase of intracellular Ca^{2+} (Fig. 5). Two minutes after application of osmotic stress the intracellular Ca^{2+} was increased significantly by 17 %. In the presence of 20 µM SKF96365 the fluorescence increase amounted to only 4 %. Similarly, 2 min of heat (52 °C) application resulted in a significant increase of fluorescence by 23 %, which was reduced to 10 % by SKF96365. Also the laser light stimulation resulted in fluorescence increase (37 %); the inhibition by SKF96365 was not as effective as after osmotic stress or heat, but nevertheless significant (p<0.01).

Discussion

Mast cells express TRPV proteins

Western blot and RT-PCR analysis revealed than TRPV1, TRPV2 and TRPV4 are expressed in the HMC-1. The multiple bands are characteristic for TRPV glycoprotein (Kedei *et al.* 2001). We could confirm these well known characteristics by treatment of HMC-1 cell lysates with PNGase F and Endo H (data not shown). Our results are in agreement with previous investigations on TRPV1 and TRPV2 (Kedei *et al.* 2001, Jahnel *et al.* 2003, Barnhill *et al.* 2004). In contrast to other

publications that reported two bands for TRPV4 (Vriens *et al.* 2005, Lorenzo *et al.* 2008). Figure 1A exhibits only one band.

Mast-cell degranulation is induced by mechanical stress, heat and red light

Mechanical and thermal stimuli have been shown to induce Ca^{2+} entry in rat basophilic leukemia (RBL) cells *via* activation of TRPV2 (Stokes *et al.* 2004). Here we demonstrate that application of physical stimuli to the human mast cells HMC-1 also induced degranulation (see in particular the SKF96365-sensitive histamine release, Table 2). Mast cell degranulation was observed in response to mechanical stress (applied as pressure gradient across the cell membrane) and heat with temperatures of bath solution exceeding 50 °C, as well as laser light of 640 nm wavelength. Degranulation was blocked by DSCG (Zhang *et al.* 2008) or RuR, an inhibitor of the TRPV channel family, and by SKF96365, an inhibitor specific for TRPV2 among the TRPV family (Clapham 2009); we therefore suggest that the degranulation induced by the physical stimuli may be attributed to activation of TRPV2, which is expressed in the HMC-1 (Fig. 1). The fact that in the presence of the inhibitor SKF96365 the physical stimuli, in particular noxious heat, could induce only reduced degranulation supports the notion that activation of TRPV2 is involved in the observed degranulation processes.

TRPV2-mediated current is activated by mechanical stress, heat and red light

All three physical stimuli induced a conductance increase; activation of the current could be inhibited by 10 µM RuR. That indeed TRPV2 was involved was again demonstrated by the application of the TRPV2-specific inhibitor SKF96365, which blocked the pressure-gradient- and also the laser-induced currents. In favour of TRPV2 activation by the mechanical stress is also the relatively low selectivity ratio of about 4 for divalent cations, compared to monovalent ones, calculated from the reversal potential. Other members of the TRPV family exhibit higher selectivity ratios (Clapham 2009). For the heat-induced current, its activation only at temperatures exceeding 50 °C is also a clear indication for the activation of TRPV2. Influx of extracellular Ca^{2+} through TRPV channels has been demonstrated to form a key step preceding mast-cell degranulation (Stokes *et al.* 2004, Yang *et al.* 2007). We believe that the increase in TRPV2-mediated current is due to channel activation

rather than TRPV2 expression since the responses a fast and reversible. Figure 2A e.g. illustrates the fast onset in response to mechanical stress and desensitation even during maintained stress.

In the rat mast-cell line RBL-2H3, laser irradiation at 532 nm and a power density of about 0.14 W/cm^2 induced degranulation with histamine release reaching saturation after about 20 min (Yang *et al.* 2007). The irradiation also resulted in an increase in intracellular Ca^{2+} activity; since the application of RuR could block the light-induced histamine release, the authors conclude that TRPV4 was activated. In the RBL-2H3 cells the isoforms TRPV1, 2 and 6 are also expressed (Stokes *et al.* 2004). Since RuR is not specific for TRPV4 their conclusion needs further justification, and the activation of another channel, for instance TRPV2, cannot be excluded. On the other hand our irradiation parameters with 640 nm wavelength and 6 W/cm^2 power density are clearly different to those used in the studies discussed above.

It has recently been shown (Neeper *et al.* 2007) that the expression of murine TRPV2 expressed in HEK293 cells can be activated by temperatures exceeding 52 °C, but not the human isoform of TRPV2. The authors discuss that this might be a species difference of TRPV2, possibly involving species differences in the regulatory mechanisms involved. Our results clearly demonstrate that the human TRPV2 in the HMC-1 can be activated by temperatures above 50 °C. A TRPV2-PKA signalling pathway has been demonstrated in mast cells (Stokes *et al.* 2004), and regulatory mechanisms seem to be involved in the heat responsiveness of TRPV1 (Prescott and Julius 2003) and TRPV4 (Watanabe *et al.* 2002).

The data we have obtained in the present study demonstrate for the first time that red laser light can induce mast cell degranulation, and that an essential role in this process is played by the activation of an ion channel that is most likely TRPV2. All three types of physical stimuli: light, mechanical stress and noxious heat, activated TRPV2 leading to increased intracellular Ca^{2+} levels and to mast cell degranulation. This is consistent with the previously demonstrated TRPV2-activation induced Ca^{2+} entry (Stokes *et al.* 2004). Mast-cell degranulation can also be induced by Ca^{2+} entry, using the Ca^{2+} ionophore A23187 (Ahrens *et al.* 2003).

Despite the importance of TRPV2 other ion channels may also become activated by the physical stimuli. The mechanical stress-induced currents cannot completely be inhibited by RuR, and at least a current component may be mediated by Cl$^-$ channels (Fig. 2F),

possibly of the ClC family, as has previously been described in mast cells (Duffy *et al.* 2001, Kulka *et al.* 2002). The presence of a stress-activated, DIDS-sensitive Cl$^-$ channel in HMC-1 has recently been demonstrated (Wang *et al.* 2009).

The three physical stimuli studied here are also employed in Traditional Chinese Medicine to treat various diseases. These include mechanical stress in conventional acupuncture, heat reaching temperatures high enough to induce TRPV2 activation during moxibustion (Zhang and Wu 2006), and more recently the successful use of "laser-needle" acupuncture (Litscher and Schikora 2007). Given that it has already been demonstrated that acupuncture-induced mast-cell degranulation can be correlated with pain suppression (Zhang *et al.* 2008), TRPV2 might be an input receptor.

Conflict of Interest

There is no conflict of interest.

Acknowledgements

References

AHRENS F, GÄBEL G, ASCHENBACHL JR: A23187-activated mast cells affect intestinal function in the pig proximal colon – role for prostaglandins. *Inflamm Res* **52** (Suppl): S15-S16, 2003.

BARNHILL JC, STOKES AJ, KOBLAN-HUBERSON M, SHIMODA LM, MURAGUCHI A, ADRA CN, TURNER H: RGA protein associates with a TRPV ion channel during biosynthesis and trafficking. *J Cell Biochem* **91**: 808-820, 2004.

BÍRÓ T, MAURER M, MODARRES S, LEWIN NE, BRODIE C, ÁCS G, ÁCS P, PAUS R, BLUMBERG PM: Characterization of functional vanilloid receptors expressed by mast cells. *Blood* **91**: 1332-1340, 1998.

BRADDING P, OKAYAMA Y, KAMBE N, SAITO H: Ion channel gene expression in human lung, skin, and cord blood-derived mast cells. *J Leukoc Biol* **73**: 614-620, 2003.

BUTTERFIELD JH, WEILER D, DEWALD G, GLEICH GJ: Establishment of an immature mast cell line from a patient with mast cell leukemia. *Leuk Res* **12**: 345-355, 1988.

CLAPHAM D: Transient receptor potential (TRP) channels. In: *Encyclopedia of Neuroscience*. RL SQUIRE (ed.), Academic Press, Oxford, 2009, pp 1109-1133.

DUFFY SM, LEYLAND ML, CONLEY EC, BRADDING P: Voltage-dependent and calcium-activated ion channels in the human mast cell line HMC-1. *J Leukoc Biol* **70**: 233-240, 2001.

ESHKEVARI L: Acupuncture and pain: a review of the literature. *AANA J* **71**: 361-370, 2003.

GUNTHORPE MJ, BENHAM CD, RANDALL A, DAVIS JB: The diversity in the vanilloid (TRPV) receptor family of ion channels. *Trends Pharmacol Sci* **23**: 183-191, 2002.

JAHNEL R, BENDER O, MÜNTER LM, DREGER M, GILLEN C, HUCHO F: Dual expression of mouse and rat VRL-1 in the dorsal root ganglion derived cell line F-11 and biochemical analysis of VRL-1 after heterologous expression. *Eur J Biochem* **270**: 4264-4271, 2003.

KEDEI N, SZABO T, LILE JD, TREANOR JJ, OLAH Z, IADAROLA MJ, BLUMBERG PM: Analysis of the native quaternary structure of vanilloid receptor 1. *J Biol Chem* **276**: 28613-28619, 2001.

KULKA M, SCHWINGSHACKL A, BEFUS AD: Mast cells express chloride channels of the ClC family. *Inflamm Res* **51**: 451-456, 2002.

LITSCHER G: Modernization of acupuncture using high-tech methods at the TCM Research Center Graz - Teleacupuncture bridges science and practice. In: *Current Research in Acupuncture (Research Monograph)*. Y XIA, GH DING, GC WU (eds), Chapter 22, Springer, New York, 2012.

LITSCHER G, SCHIKORA D: *Laserneedle - Acupuncture: Science and Practice*. Pabst Science Publishers, Lengerich, Berlin, Bremen, 2007.

LITSCHER G, WANG L, WIESNER-ZECHMEISTER M: Specific effects of laserpuncture on the cerebral circulation. *Lasers in Medical Science* **15**: 57-62, 2000.

LORENZO IM, LIEDTKE W, SANDERSON MJ, VALVERDE MA: TRPV4 channel participates in receptor-operated calcium entry and ciliary beat frequency regulation in mouse airway epithelial cells. *Proc Natl Acad Sci USA* **105**: 12611-12616, 2008.

NEEPER MP, LIU Y, HUTCHINSON TL, WANG Y, FLORES CM, QIN N: Activation properties of heterologously expressed mammalian TRPV 2: evidence for species dependence. *J Biol Chem* **282**: 15894-15902, 2007.

NUMAZAKI M, TOMINAGA M: Nociception and TRP channels. *Curr Drug Targets CNS Neurol Disord* **3**: 479-485, 2004.

OWSIANIK G, TALAVERA K, VOETS T, NILIUS B: Permeation and selectivity of TRP channels. *Annu Rev Physiol* **68**: 685-717, 2006.

PRESCOTT ED, JULIUS D: Modular PIP_2 binding site as a determinant of capsaicin receptor sensitivity. *Science* **300**: 1284-1288, 2003.

RAMSEY IS, DELLING M, CLAPHAM DE: An introduction to TRP channels. *Annu Rev Physiol* **68**: 619-647, 2006.

STOKES AJ, SHIMODA LMN, KOBLAN-HUBERSON M, ADRA CN, TURNER H: A TRPV2-PKA signaling module for transduction of physical stimuli in mast cells. *J Exp Med* **200**: 137-147, 2004.

SUDO N, TANAKA K, KOGA Y, OKUMURA Y, KUBO C, NOMOTO K: Extracellular ATP activates mast cells via a mechanism that is different from the activation induced by the cross-linking of Fc receptors. *J Immunol* **156**: 3970-3979, 1996.

VRIENS J, OWSIANIK G, FISSLTHALER B, SUZUKI M, JANSSENS A, VOETS T, MORISSEAU C, HAMMOK BD, FLEMING I, BUSSE R, NILIUS B: Modulation of Ca^{2+} permeable cation channel TRPV4 by cytochrome P450 epoxygenases in vascular endothelium. *Circ Res* **97**: 908-915, 2005.

WANG L, DING G, GU Q, SCHWARZ W: Single-channel properties of a stretch-sensitive chloride channel in the human mast cell line HMC-1. *Eur Biophys J* **39**: 757-767, 2010.

WATANABE H, VRIENS J, SUH SH, BENHAM CD, DROOGMANS G, NILIUS B: Heat-evoked activation of TRPV4 channels in a HEK293 cell expression system and in native mouse aorta endothelial cells. *J Biol Chem* **277**: 47044-47051, 2002.

YANG WZ, CHEN JY, YU JT, ZHOU LW: Effects of lower power laser irradiation on intracellular calcium and histamine release in RBL-2H3 mast cells. *Photochem Photobiol* **83**: 979-984, 2007.

ZHANG D, DING G, SHEN X, YAO W, ZHANG Z, ZHANG Y, GU Q: Role of mast cells in acupuncture effects: A pilot study. *Explore J Sci Heating* **4**: 170-177, 2008.

ZHANG D, DING GH, SCHWARZ W: Cellular mechanisms in acupuncture-induced mast cell degranulation. *J Altern Complem Med* **13**: 899, 2007a.

ZHANG D, SPIELMANN A, DING GH, SCHWARZ W: Role of mast cells as peripheral target in acupuncture and moxibustion. In: *Scientific Approaches to Chinese Medicine.* Heidelberg School Edition, 2007b, pp 87-89.

ZHANG JF, WU YC: Modern progress of mechanism of moxibustion therapy. *J Acupunct Tuina Sci* **4**: 257-260, 2006.